



ARTICLE OPEN

CD137 costimulation enhances the antiviral activity of V γ 9V δ 2-T cells against influenza virus

Yujun Pei¹, Kun Wen¹, Zheng Xiang¹, Chunyu Huang¹, Xiwei Wang¹, Xiaofeng Mu¹, Liyan Wen¹, Yiping Liu¹ and Wenwei Tu¹

Influenza epidemics and pandemics are constant threats to global public health. Although strategies including vaccines and antiviral drugs have achieved great advances in controlling influenza virus infection, the efficacy of these strategies is limited by the highly frequent mutations in the viral genome and the emergence of drug-resistant strains. Our previous study indicated that boosting the immunity of human V γ 9V δ 2-T cells with the phosphoantigen pamidronate could be a therapeutic strategy to treat seasonal and avian influenza virus infections. However, one notable drawback of $\gamma\delta$ -T cell-based immunotherapy is the rapid exhaustion of proliferation and effector responses due to repeated treatments with phosphoantigens. Here, we found that the expression of CD137 was inducible in V γ 9V δ 2-T cells following antigenic stimulation. CD137⁺ V γ 9V δ 2-T cells displayed more potent antiviral activity against influenza virus than their CD137⁻ counterparts in vitro and in Rag2^{-/-} γ c^{-/-} mice. We further demonstrated that CD137 costimulation was essential for V γ 9V δ 2-T cell activation, proliferation, survival and effector functions. In humanized mice reconstituted with human peripheral blood mononuclear cells, CD137 costimulation with a recombinant human CD137L protein boosted the therapeutic effects of pamidronate against influenza virus. Our study provides a novel strategy of targeting CD137 to improve the efficacy of V γ 9V δ 2-T cell-based immunotherapy.

Signal Transduction and Targeted Therapy (2020)5:74

; <https://doi.org/10.1038/s41392-020-0174-2>

INTRODUCTION

Influenza is an acute respiratory virus infection that continues to pose epidemic, zoonotic and pandemic threats to global human health with significant morbidity and mortality.^{1,2} Although strategies including vaccines and antiviral drugs have achieved great advances in controlling influenza virus infection, the efficacy of these strategies is still limited by the highly frequent mutations in the viral genome and emergence of drug-resistant strains.^{3–5} A strategy to boost host innate immunity was recently thought to have obvious advantages in controlling influenza infection without the risks of viral mutation and antiviral resistance.^{6–8}

$\gamma\delta$ -T cells, as innate-like T lymphocytes, represent a minor but crucial population in the immune system.^{9–12} Most $\gamma\delta$ -T cells in the peripheral blood and lymphoid organs of healthy human adults are V γ 9V δ 2-T cells. V γ 9V δ 2-T cells can be specifically activated in an HLA-unrestricted manner by small nonpeptidic phosphoantigens, which are metabolites of isoprenoid biosynthesis pathways.¹³ Pharmacological compounds, such as the aminobisphosphonates pamidronate (PAM) and zoledronate, which are commonly used for the treatment of osteoporosis and Paget's disease, can induce the activation and expansion of human V γ 9V δ 2-T cells.^{11,14,15} Previously, we demonstrated that phosphoantigen-activated V γ 9V δ 2-T cells have antiviral activities against human and avian influenza viruses mediated by killing virus-infected monocyte-derived macrophages (MDMs), inhibiting virus replication, and promoting the production of virus-specific antibodies.^{16–20} Recently, we further reported that PAM can control influenza diseases by expanding the V γ 9V δ 2-T cell population in humanized

mice.^{21,22} However, the application of PAM for the treatment of influenza is limited by the rapid exhaustion of the proliferation and effector responses of V γ 9V δ 2-T cells resulting from repeated treatments with the phosphoantigens. Although the underlying mechanisms of this exhaustion are still not clear, the suboptimal stimulation or lack of optimal costimulation may explain it. Therefore, detailed characterizations of the costimulatory factors required for sustained activation and survival of V γ 9V δ 2-T cells are required to solve this problem.²³

CD137 (4-1BB; TNFRSF9), a membrane-bound receptor that belongs to the tumor necrosis factor receptor superfamily, is an inducible T cell costimulatory molecule.²⁴ The interaction of CD137 with its major ligand, CD137L, has been shown to result in the survival, expansion, and differentiation of $\alpha\beta$ -T cells, particularly CD8⁺ T cells, into effectors and the establishment of long-term memory.^{25–27} Agonistic anti-CD137 monoclonal antibodies (mAbs) have been shown to enhance the efficacy of vaccines against influenza virus and poxvirus by enhancing CD8⁺ or CD4⁺ T cell responses.^{28,29} However, whether CD137 has similar costimulatory effect on $\gamma\delta$ -T cells remains unknown.

In this study, we demonstrated critical roles for CD137-CD137L interactions in the proliferation, survival and effector functions of V γ 9V δ 2-T cells in response to influenza virus infection in vitro and in vivo. Using a recombinant human SA-hCD137L protein containing the extracellular domains of human CD137L (hCD137L) fused to a core streptavidin (SA) molecule, we demonstrated that SA-hCD137L is an efficient adjuvant for PAM therapy for influenza virus infection that functions by improving the antiviral activity of human V γ 9V δ 2-T cells in humanized mice. Our study suggests the

¹Department of Paediatrics and Adolescent Medicine, Li Ka Shing Faculty of Medicine, The University of Hong Kong, Hong Kong, China

Correspondence: Wenwei Tu (wwtu@hku.hk)

These authors contributed equally: Yujun Pei, Kun Wen

Received: 30 January 2020 Revised: 14 April 2020 Accepted: 14 April 2020

Published online: 03 June 2020

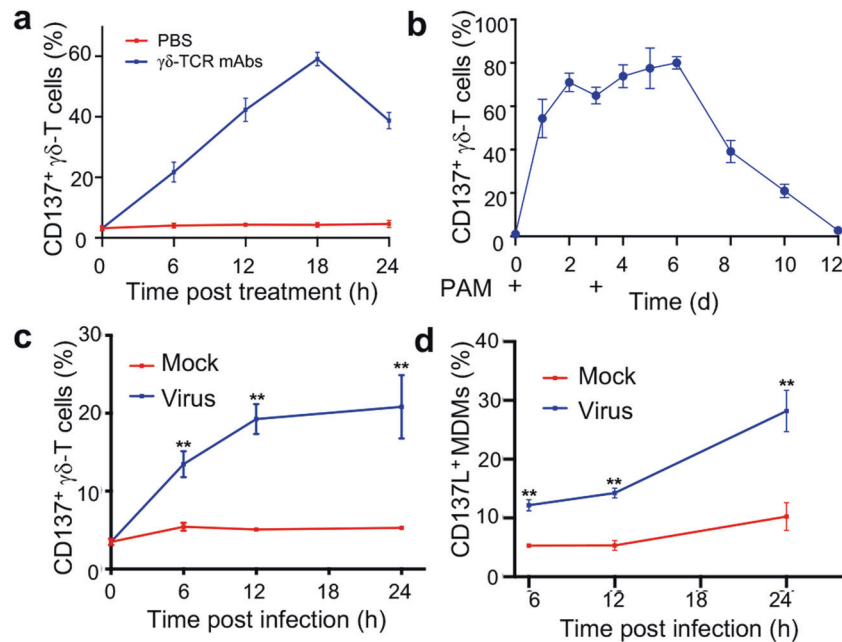


Fig. 1 Influenza virus induced CD137 and CD137L expression on Vγ9Vδ2-T cells and MDMs, respectively. **a** The expression of CD137 on Vγ9Vδ2-T cells was detected by flow cytometry upon stimulation with or without an anti-γδ-TCR mAb for the indicated time. **b** CD137 expression on human Vγ9Vδ2-T cells was detected at the indicated time during ex vivo expansion of Vγ9Vδ2-T from huPBMC with PAM. **c** CD137 expression on Vγ9Vδ2-T cells was detected during coculture with mock- or influenza virus-infected autologous MDMs for the indicated time. **d** CD137L expression on MDMs was evaluated during mock or influenza virus infection. Cells were harvested at the indicated time and assessed by flow cytometry for CD137 or CD137L expression. The percentages of CD137⁺ cells in Vγ9Vδ2-T cells and CD137L⁺ cells in MDMs are shown (mean ± SEM). **p* < 0.05; ***p* < 0.01

novel strategy of targeting CD137 to improve the antiviral activity of human Vγ9Vδ2-T cells.

RESULTS

Influenza virus induced CD137 and CD137L expression on Vγ9Vδ2-T cells and MDMs, respectively

To understand the effect of the CD137/CD137L interaction on the antiviral activity of Vγ9Vδ2-T cells, we first analyzed CD137 expression on human Vγ9Vδ2-T cells upon γδ-TCR activation in vitro. As shown in Fig. 1a, CD137 was expressed at very low levels on resting Vγ9Vδ2-T cells, but its expression was upregulated, peaked at 18 h and then decreased following activation by anti-γδ-TCR mAbs. PAM could also induce the expression of CD137 when used for ex vivo expansion of Vγ9Vδ2-T cells (Fig. 1b). We then detected the expression of CD137 on Vγ9Vδ2-T cells while coculturing PAM-expanded Vγ9Vδ2-T cells with influenza H1N1/A/PR/8/34 virus-infected autologous MDMs. CD137 was rapidly induced in Vγ9Vδ2-T cells, and approximately 20% of the Vγ9Vδ2-T cells became CD137⁺ cells after 24 h of coculture with influenza virus-infected MDMs (Fig. 1c). Importantly, CD137L expression was also rapidly upregulated in MDMs, and 25.7 ± 4.3% of the MDMs became CD137L⁺ cells after 24 h of influenza virus infection (Fig. 1d). These data indicated that the levels of CD137 and CD137L were upregulated on Vγ9Vδ2-T cells and MDMs, respectively, during influenza virus infection, raising the possibility that CD137/CD137L could serve as an effective costimulatory signaling pair to promote the antiviral activity of Vγ9Vδ2-T cells.

CD137⁺ Vγ9Vδ2-T cells had more potent antiviral activity against influenza virus than their CD137⁻ counterparts in vitro

We further compared the phenotype and function of CD137⁺ and CD137⁻ Vγ9Vδ2-T cells during coculture with influenza virus-infected MDMs. As shown in Fig. 2a, CD137⁺ Vγ9Vδ2-T cells expressed higher levels of activation markers (CD25, CD69 and

NKG2D) and cell death-related receptor ligands (Fas, FasL and TRAIL) than their CD137⁻ counterparts. Importantly, the expression of CD107a, a marker associated with the degranulation of NK cells and cytotoxic T lymphocytes (CTLs),³⁰ was significantly higher in CD137⁺ Vγ9Vδ2-T cells than CD137⁻ Vγ9Vδ2-T cells after coculture with influenza virus-infected MDMs (Fig. 2a), which suggested that influenza virus-infected MDMs triggered more intensive granule release from CD137⁺ Vγ9Vδ2-T cells than from their CD137⁻ counterparts. Furthermore, CD137⁺ Vγ9Vδ2-T expressed dramatically more cytolytic granule molecules (perforin and granzyme B) and antiviral cytokines (IFN-γ) than their CD137⁻ counterparts (Fig. 2b). These data indicated that CD137⁺ Vγ9Vδ2-T cells had a superior activation status and should have much higher antiviral activities than CD137⁻ Vγ9Vδ2-T cells.

To further compare the antiviral activities of CD137⁺ and CD137⁻ Vγ9Vδ2-T cells, we sorted these two subsets and detected their cytotoxic activity against influenza virus-infected MDMs. As shown in Fig. 2c, both CD137⁺ and CD137⁻ Vγ9Vδ2-T cells could efficiently kill virus-infected cells, but the CD137⁺ Vγ9Vδ2-T cells displayed superior cytotoxic activity toward virus-infected cells. These data demonstrated that CD137 expressed on Vγ9Vδ2-T cells could be a useful marker for identifying the γδ-T cell subset with superior activation and antiviral activity.

CD137⁺ Vγ9Vδ2-T cells had more potent antiviral activity than their CD137⁻ counterparts in vivo

To further confirm the antiviral activities of both CD137⁺ and CD137⁻ Vγ9Vδ2-T cells against influenza virus in vivo, Rag2^{-/-} γc^{-/-} mice were infected with influenza virus intranasally (i.n.). CD137⁺ and CD137⁻ Vγ9Vδ2-T cell subsets were sorted after activation by an anti-γδ-TCR antibody in vitro, and then highly purified (>95%) CD137⁺, CD137⁻ or whole Vγ9Vδ2-T cells were adoptively transferred into the influenza virus-infected mice on days 2, 4, and 6 post infection (Fig. 3a). Consistent with our previous results,²¹ adoptive transfer of whole Vγ9Vδ2-T cells significantly reduced weight loss and mortality (Fig. 3b).

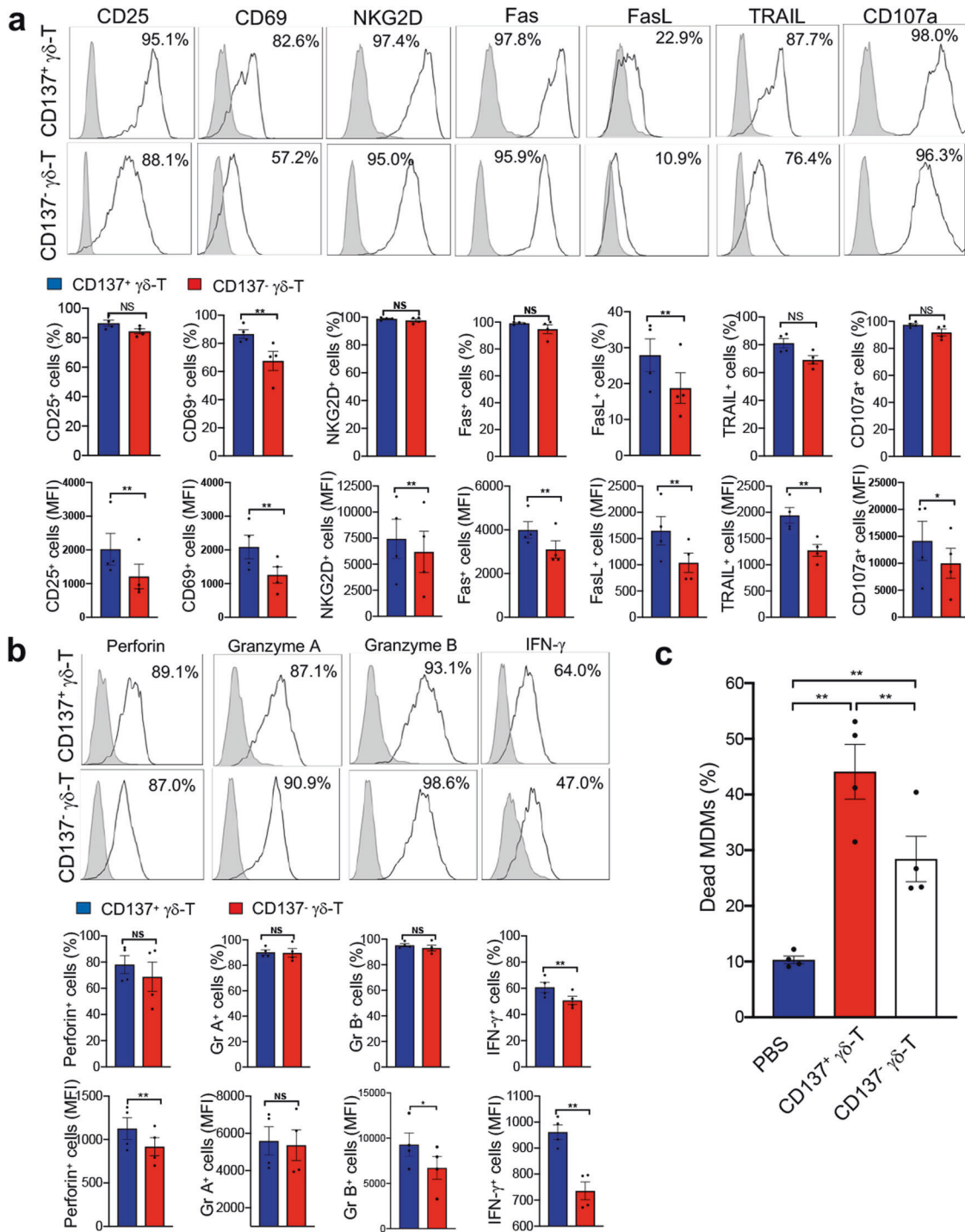


Fig. 2 CD137⁺ Vγ9Vδ2-T Cells had more potent antiviral activity against influenza virus than their CD137⁻ counterparts in vitro. **a, b** Human MDMs were infected with influenza virus at an MOI of 2 for 1h and then cocultured with PAM-expanded autologous Vγ9Vδ2-T cells for 12h at a ratio of 1:1. The indicated markers were detected by flow cytometry with surface (**a**) or intracellular (**b**) staining. Representative histograms (above) depict the positive percentage for the indicated markers (blank histogram), with shaded histograms representing isotype controls. The percentages and mean fluorescence intensities (MFIs) of positive cells are shown in the bar graphs (underneath) as the mean ± SEM. **c** CD137⁺ and CD137⁻ Vγ9Vδ2-T cells were separated from PAM-expanded Vγ9Vδ2-T cells with magnetic beads after stimulation with an anti-γδ-TCR mAb (0.5 μg/ml) for 6h. Then, these cells (effector cells, E) were cocultured with influenza virus-infected autologous MDMs (target cells, T) at an E:T ratio of 10:1 for 6h. Cytotoxicity was calculated as the proportion of dead MDMs. Data shown in the bar graphs are the mean ± SEM. **p* < 0.05; ***p* < 0.01

Treatment with CD137⁺ Vγ9Vδ2-T cells showed more efficacy in controlling influenza disease than CD137⁻ and whole Vγ9Vδ2-T cells, with the CD137⁺ Vγ9Vδ2-T cells producing the lowest weight loss (Fig. 3b), highest survival rate (Fig. 3c) and attenuated

lung inflammation (Fig. 3d). Furthermore, CD137⁺ Vγ9Vδ2-T cell treatment showed a better ability to reduce virus titers in the lungs of infected mice by day 8 post infection than either CD137⁻ T cells or whole Vγ9Vδ2-T cells (Fig. 3e). These data demonstrated

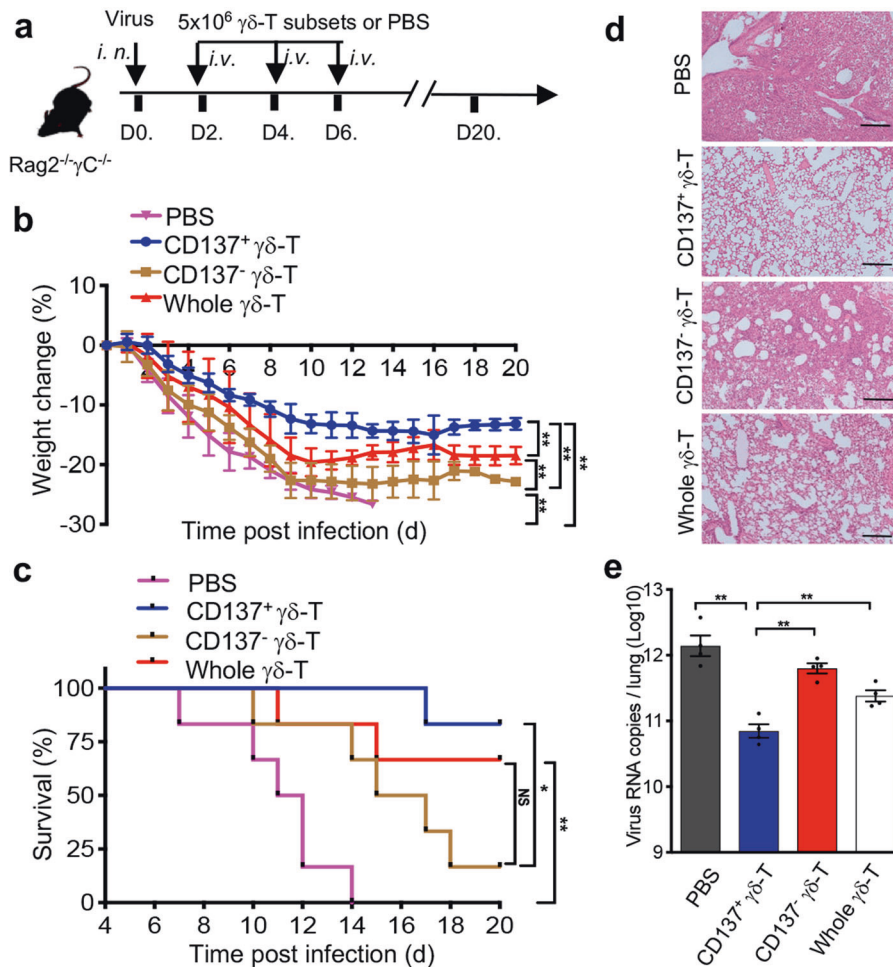


Fig. 3 CD137⁺ Vγ9Vδ2-T cells had more potent antiviral activity than their CD137⁻ counterparts in vivo. **a** Protocol for evaluation of the therapeutic effect of Vγ9Vδ2-T cell subsets on influenza virus-infected Rag2^{-/-} γC^{-/-} mice. Rag2^{-/-} γC^{-/-} mice were infected with a sublethal dose of influenza virus (25 μl, 10⁴ TCID₅₀) intranasally (i.n.) on day 0. Highly purified CD137⁺, CD137⁻ or whole Vγ9Vδ2-T cells (5 × 10⁶ cells/mouse) or the same volume of PBS was adoptively transferred intravenously (i.v.) into virus-infected mice at the indicated time. **b, c** The body weight changes (**b**) and survival (**c**) of virus-infected mice were measured at the indicated time. **d, e** Lung tissues from infected mice were collected on day 8 post infection for histological analysis and viral load testing. Histological sections were stained with hematoxylin and eosin (**d**). Bars, 100 μm; the number of viral RNA copies in the lungs (**e**) was determined by RT-PCR. Error bars indicate the mean ± SEM. **p* < 0.05; ***p* < 0.01; ns, no significant difference

that CD137⁺ Vγ9Vδ2-T cells displayed superior antiviral effects in controlling influenza disease in vivo.

CD137 costimulation enhanced the antiviral activity of Vγ9Vδ2-T cells against influenza virus

We have shown that CD137⁺ Vγ9Vδ2-T cells display more potent antiviral activity than their CD137⁻ counterparts in vitro and in vivo. To determine whether CD137 costimulation is involved in the antiviral activity of Vγ9Vδ2-T cells, a recombinant SA-hCD137L protein containing the extracellular domains of human CD137L (hCD137L) fused to a core streptavidin (SA) molecule was generated. The addition of the recombinant SA-hCD137L protein to a coculture of whole Vγ9Vδ2-T cells with influenza virus-infected MDMs significantly enhanced the expression of CD107a, cytolytic granule molecules (perforin and granzyme B) and an antiviral cytokine (IFN-γ) in the Vγ9Vδ2-T cells (Fig. 4a). In contrast, there were no significant changes in the expression of CD25, CD69, FasL and TRAIL after treatment with the recombinant SA-hCD137L protein (Fig. 4a). Similar to that induced by costimulation with an anti-CD137 agonistic mAb, the increased expression of CD107a induced by costimulation with SA-hCD137L was completely abrogated when CD137/CD137L signaling was blocked

with an anti-CD137 antagonistic mAb (Supplemental Fig. 1). These data confirmed that the SA-CD137L protein could specifically activate the CD137/CD137L pathway. Importantly, the recombinant protein significantly increased the cytotoxicity of Vγ9Vδ2-T cells against influenza virus-infected MDMs (Fig. 4b). These data demonstrated that CD137 engagement was important for the antiviral activity of Vγ9Vδ2-T cells.

To further confirm the costimulatory role of CD137 in the antiviral activity of Vγ9Vδ2-T cells against influenza virus, an anti-CD137 neutralizing mAb was used to block CD137 signaling when Vγ9Vδ2-T cells were cocultured with virus-infected MDMs. The blockade of CD137 signaling significantly decreased the expression of CD107a, cytolytic granule molecules (perforin and granzyme B) and an antiviral cytokine (IFN-γ) in the Vγ9Vδ2-T cells (Fig. 4c). In contrast, there were no significant changes in the expressions of CD25, CD69, TRAIL and FasL after treatment with the anti-CD137 neutralizing mAb (Fig. 4c). Moreover, compared with PBS or mlgG1 treatment, blocking CD137 significantly abrogated the cytolytic activity of Vγ9Vδ2-T cells against H1N1-infected MDMs (Fig. 4d). Taken together, these data demonstrated that CD137 costimulation could enhance the antiviral activity of Vγ9Vδ2-T cells against influenza virus.

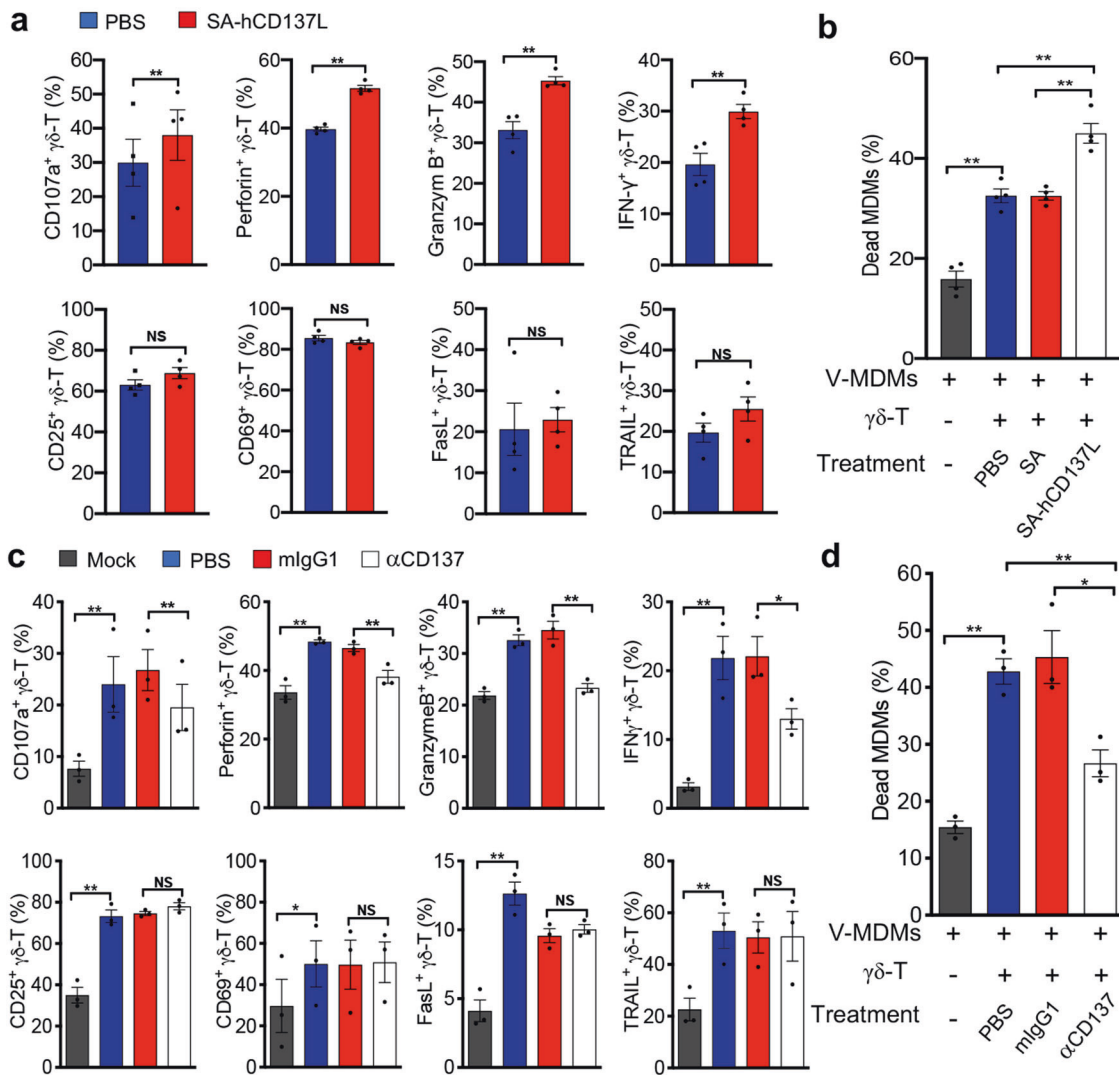


Fig. 4 CD137 costimulation enhanced the antiviral activity of V γ 9V δ 2-T cells against influenza virus. Human MDMs (target cells, T) were infected with PR8 (V-MDMs) at an MOI of 2 for 1h and then cocultured with PAM-expanded autologous V γ 9V δ 2-T cells (effector cells, E) at an E: T ratio of 10:1 for 6h with the indicated treatment. **a** V-MDMs cocultured with V γ 9V δ 2-T cells in the presence of SA-hCD137L (500ng/ml) or PBS, which was used as a control. The surface and intracellular expression of the indicated markers by V γ 9V δ 2-T cells was detected with flow cytometry. **b** The proportions of dead (EthD2⁺) MDMs were detected by flow cytometry. **c** V-MDMs were cocultured with V γ 9V δ 2-T cells in the presence of a neutralizing anti-CD137 mAb (α CD137) or isotype control (mIgG1). The surface and intracellular expression of the indicated markers by V γ 9V δ 2-T cells was detected with flow cytometry. **d** The proportions of dead (EthD2⁺) MDMs were detected by flow cytometry. Data are shown as the mean \pm SEM. * p < 0.05; ** p < 0.01; ns, no significant difference

CD137 costimulation promoted the proliferation and prolonged the survival of V γ 9V δ 2-T cells

To determine whether CD137 costimulation can promote the proliferation of V γ 9V δ 2-T cells, CD137 was blocked with a neutralizing mAb during the ex vivo expansion of V γ 9V δ 2-T cells from human peripheral blood mononuclear cells (huPBMC) induced by PAM. Compared with control treatment, blocking CD137 resulted in a significant decrease in V γ 9V δ 2-T cells in terms of both the cell frequency (Fig. 5a, b) and absolute cell number (Fig. 5c) after 7 days of expansion. Additionally, the expanded V γ 9V δ 2-T cells exhibited a statistic decrease in the proliferation index after CD137 blockade in a CFSE proliferation assay (Fig. 5d, e). To further confirm the role of CD137 costimulation in promoting the proliferation of V γ 9V δ 2-T cells, we added the recombinant SA-hCD137L protein to $\gamma\delta$ -T cells purified by positive selection and cultured the cells for 5 days in the absence or presence of IL-2. As shown in Fig. 5f, the

SA-hCD137L protein alone could not enhance the expansion of V γ 9V δ 2-T cells; however, the recombinant protein could significantly raise the absolute cell number of $\gamma\delta$ -T cells in the presence of a low dose of IL-2 (50 IU/ml), and the cells were expanded by approximately 1.4-fold after 5 days of culturing. This result indicated that CD137 costimulation could promote the proliferation of activated V γ 9V δ 2-T cells in an IL-2-dependent manner. Importantly, blockade of CD137 induced more apoptosis (21.05 \pm 0.55%, AV⁺PI⁻: early apoptosis; 27.43 \pm 1.03%, AV⁺PI⁺: late apoptosis) in V γ 9V δ 2-T cells activated by an anti- $\gamma\delta$ -TCR antibody for 24 h than did an mIgG1 control (15.35 \pm 0.32%, AV⁺PI⁻: early apoptosis; 19.30 \pm 1.70%, AV⁺PI⁺: late apoptosis) (Fig. 5g–i), which indicated that CD137 costimulation also inhibited V γ 9V δ 2-T cell apoptosis and enhanced the survival of V γ 9V δ 2-T cells. Collectively, these data demonstrated that CD137 costimulation promoted the proliferation and prolonged the survival of V γ 9V δ 2-T cells.

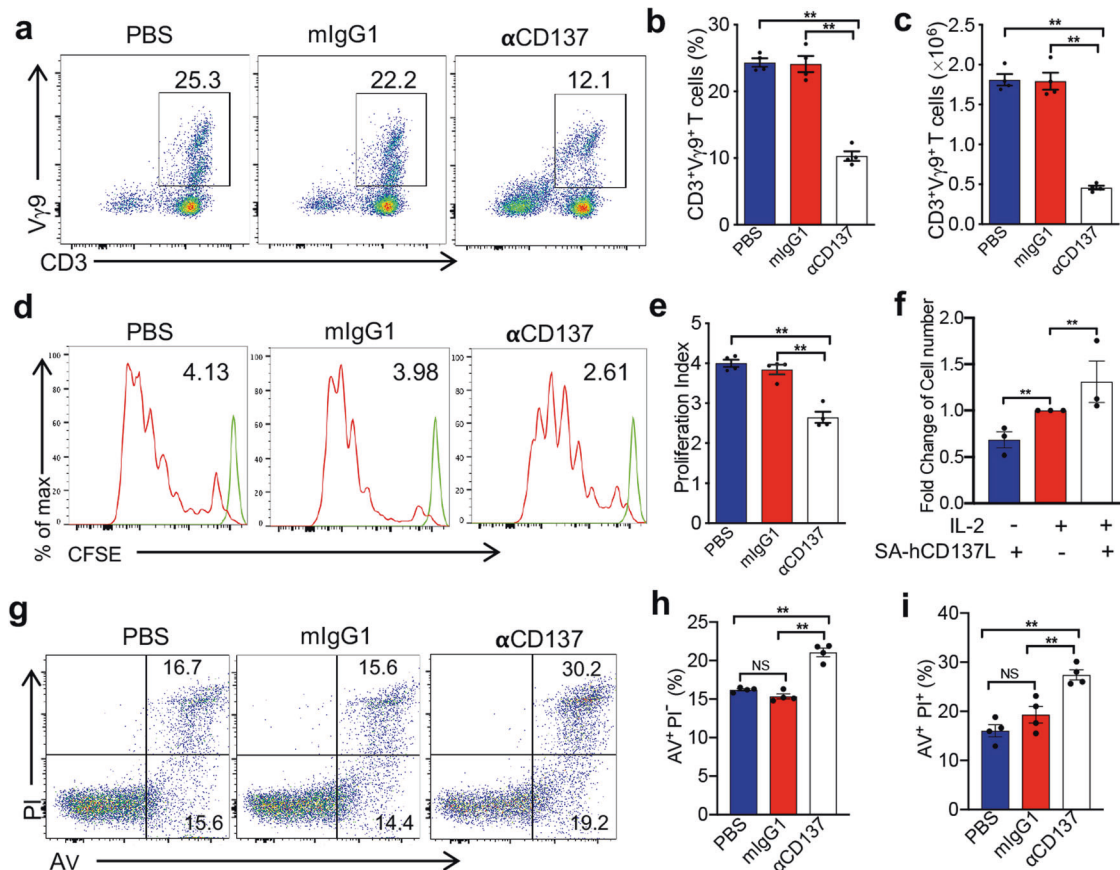


Fig. 5 CD137 costimulation promoted the proliferation and prolonged the survival of Vγ9Vδ2-T cells. **a–c** Vγ9Vδ2-T cells were expanded from huPBMC with PAM/IL-2 for 7 days in the presence of anti-CD137 neutralizing antibody (αCD137), mouse IgG1 (mlgG1) or PBS. The percentage (**a, b**) and absolute cell number (**c**) of Vγ9Vδ2-T cells were detected by flow cytometry. **d, e** Vγ9Vδ2-T cells were expanded from CFSE-labeled huPBMC with PAM/IL-2 for 7 days. **d** Representative histograms show the proliferation of CFSE-labeled Vγ9Vδ2-T cells. **e** The proliferation index was calculated with FlowJo software and is presented in bar graphs. The proliferation index is the total number of divisions divided by the number of cells that underwent division. **f** Human Vγ9Vδ2-T cells were isolated from huPBMC by positive selection and cultured with the SA-hCD137L protein (500ng/ml) or human IL-2 (50 IU/ml) in the presence of PAM (9μg/ml) for 5 days. Fold changes in the Vδ2⁺ cell number in the indicated groups compared to that in the IL-2 group were calculated by flow cytometry with counting beads. **g–i** PAM-expanded Vγ9Vδ2-T cells were purified and activated with an anti-γδ-TCR antibody (0.5μg/ml) for 24h in the presence of PBS, mlgG1 or an αCD137 antibody. Apoptosis was detected by flow cytometry with Annexin V (AV) and PI staining. The data shown in the bar graphs are the mean ± SEM. ***p* < 0.01; ns, no significant difference

CD137 costimulation improved the therapeutic effect of PAM against influenza virus infection in vivo. To demonstrate whether costimulation through CD137 can improve the therapeutic effect of PAM-expanded Vγ9Vδ2-T cells against influenza virus in vivo, humanized mice reconstituted with whole huPBMC (whole-huPBMC)^{20,21,31,32} were injected intraperitoneally (i.p.) with the recombinant SA-hCD137L protein and PAM 3 days after influenza virus infection (Fig. 6a). During the 20 days of the experimental period, compared with PAM alone, the SA-hCD137L protein in combination with PAM significantly decreased the weight loss and prolonged the survival of the virus-infected whole-huPBMC humanized mice (Fig. 6b, c). Furthermore, reduced pathological severity and decreased viral loads in the lungs were observed in virus-infected whole-huPBMC humanized mice treated with SA-hCD137L and PAM compared with mice treated with PAM alone on day 10 postinfection (Fig. 6d, e). To determine whether the effect of SA-hCD137L costimulation on the control of influenza virus infection in humanized mice was mediated by Vγ9Vδ2-T cells, humanized mice reconstituted with Vγ9Vδ2-T-cell-depleted huPBMC were also included (Fig. 6a). As shown in Fig. 6, there were no therapeutic improvements achieved by administering SA-hCD137L to virus-infected humanized mice without Vγ9Vδ2-T cells. These data demonstrated that the recombinant

SA-hCD137L protein had a synergistic effect with PAM to control influenza disease in vivo and that their antiviral activity against influenza virus was mainly mediated by Vγ9Vδ2-T cells.

DISCUSSION

The ability of CD137 signaling to evoke robust αβ-T cell effector responses has been extensively demonstrated in infectious disease models. However, the role of CD137 signaling in Vγ9Vδ2-T cells remains poorly understood in the context of influenza virus infection. In this study, we demonstrate for the first time that CD137 ligation enhances Vγ9Vδ2-T cell proliferation, survival and antiviral activity against influenza virus. The CD137⁺ Vγ9Vδ2-T cell population exhibited an enhanced capability to treat influenza when employed as an adoptive γδ-T cell therapy. Furthermore, we demonstrated that a tetrameric form of a recombinant human CD137L protein, SA-hCD137L, could boost the effect of PAM therapy on influenza by costimulating Vγ9Vδ2-T cells. Our study provides a relatively effective strategy to treat influenza virus by targeting CD137 to improve the antiviral activity of human Vγ9Vδ2-T cells.

Several studies have shown that CD137 plays a critical role in αβ-T cell-mediated antiviral immune responses against influenza,^{33,34}

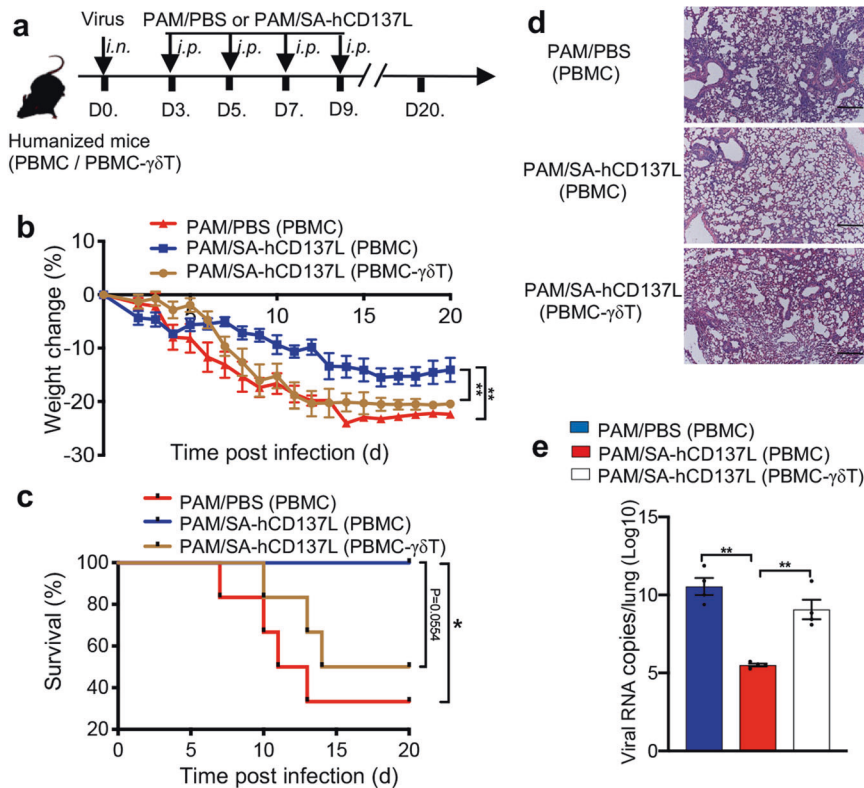


Fig. 6 CD137 costimulation improved the therapeutic effect of PAM on influenza virus infection in vivo. **a** Protocol for evaluation of the synergistic therapeutic effect of PAM and SA-hCD137L on influenza virus-infected humanized mice. Humanized mice reconstituted with whole huPBMC (PBMC) or V γ 9V δ 2-T cell-depleted huPBMC (PBMC- $\gamma\delta$ T) were infected with a sublethal dose of influenza virus (25 μ l, 10⁴ TCID₅₀) intranasally (*i.n.*), and then treated with PAM/SA-CD137 or PAM/PBS on days 3, 5, 7 and 9 post infection. **b**, **c** The body weight changes (**b**) and survival (**c**) of influenza virus-infected humanized mice were measured at the indicated time after infection. **d**, **e** Lung tissues from infected mice were collected on day 10 post infection for histological analysis and viral load testing. Histological sections were stained with hematoxylin and eosin, and representative histopathological changes are shown (**d**). Bars, 100 μ m; the number of viral RNA copies in the lungs (**e**) was determined by RT-PCR. Error bars indicate the mean \pm SEM. * p < 0.05; ** p < 0.01

hepatitis C, cytomegalovirus, HIV, lymphocytic choriomeningitis virus, and poxviruses.³⁵ As shown in previous reports on $\alpha\beta$ -T cells, CD137 signaling can inhibit activation-induced cell death (AICD), promote cell proliferation and survival, and enhance effector cell function.³⁶ Here, we also found that engagement of CD137 could provide costimulatory signals to V γ 9V δ 2-T cells to enhance proliferation, inhibit apoptosis and increase antiviral activity in vitro and in vivo, suggesting that CD137 can provide costimulatory signals to both $\alpha\beta$ - and $\gamma\delta$ -T cells.

Although previous reports have shown that CD137 is expressed on human $\gamma\delta$ -T cells,³⁷ direct comparison of the effector functions of CD137⁺ and CD137⁻ V γ 9V δ 2-T cell fractions has not been performed. Here, we found that CD137⁺ V γ 9V δ 2-T cells displayed more potent antiviral activity than their CD137⁻ counterparts in vitro and in vivo. The cytolytic phenotype of CD137⁺ effector V γ 9V δ 2-T cells suggests that CD137 may be a marker of potent effector V γ 9V δ 2-T cells (Fig. 2). Using CD137⁺ V γ 9V δ 2-T cells for adoptive cell-based therapy for influenza is superior to using CD137⁻ or whole V γ 9V δ 2-T cells (Fig. 3). These properties make adoptive transfer of CD137⁺ V γ 9V δ 2-T cells an attractive agent for the therapy of influenza diseases.

Although CD137⁺ V γ 9V δ 2-T cells expressed higher levels of activation markers (CD25, CD69 and NKG2D) and cell death-related receptor ligands (Fas, FasL and TRAIL) than their CD137⁻ counterparts (Fig. 2), there were no significant changes in the expression of CD25, CD69, TRAIL and FasL after treatment with an anti-CD137 neutralizing mAb or SA-hCD137L during coculture of PAM-expanded V γ 9V δ 2-T cells with influenza virus-infected MDMs (Fig. 4). In contrast, CD137 costimulation enhanced the

expressions of cytolytic granule molecules (perforin and granzyme B) and the antiviral cytokine IFN- γ in V γ 9V δ 2-T cells and promoted cytotoxic granule exocytosis, as marked by CD107a expression, in these cells (Fig. 4). These data indicated that the enhancement of V γ 9V δ 2-T cell effector function by CD137 costimulation was mainly mediated by the perforin/granzyme B pathway and secretion of IFN- γ .

The expression of CD137 correlates well with effective antiviral immune responses; however, anti-CD137 agonistic antibodies can induce a variety of pathologies that may limit their utility in patients.^{38,39} An alternative approach to the application of CD137-specific antibodies lies in the use of the natural CD137 ligand to stimulate antitumor T cell responses. Work from the Shirwan lab has elegantly demonstrated the therapeutic ability of a streptavidin-conjugated murine CD137L (SA-mCD137L) complex to induce effective antitumor immune responses.^{40,41} SA-mCD137L induces less lymphadenopathy and splenomegaly than antibody therapy, suggesting that SA-mCD137L has a higher therapeutic index. Here, we generated streptavidin-conjugated human CD137L protein and demonstrated that recombinant SA-hCD137L could promote the cytolytic effector function of V γ 9V δ 2-T cells against influenza-infected MDMs by promoting the release of cytolytic granules (containing perforin and granzyme B) and an antiviral cytokine (IFN- γ) from V γ 9V δ 2-T cells, suggesting that SA-hCD137L offers a compelling alternative to anti-CD137 agonistic antibody-mediated stimulation for influenza immunotherapy.

Since murine T cells do not express a homolog of the V γ 9V δ 2-TCR,¹² it was not possible to use a conventional mouse or ferret model for the study of human V γ 9V δ 2-T cells. In our previous

studies, we successfully established humanized mice containing functional human T and B cells, including a percentage of V γ 9V δ 2-T cells in the peripheral blood similar to that seen in humans.^{20,21,31,32} Moreover, we found that influenza viruses could efficiently replicate and cause pathology in these mice, indicating that the humanized mice established by us are suitable for the study of human V γ 9V δ 2-T cell immune responses to influenza viruses. Using humanized mice, we further showed the synergistic effect of PAM and recombinant SA-hCD137L against influenza virus is mediated by boosting human V γ 9V δ 2-T cell immunity.

Adoptive transfer requires the expansion and activation of autologous V γ 9V δ 2-T cells *ex vivo* and their reinfusion into patients; this approach is becoming a popular cellular immunotherapy paradigm for patients with infectious disease or cancer. The potential to expand V γ 9V δ 2-T cells *in vivo* using phosphoantigens such as PAM offers a comparatively cheaper and straightforward delivery alternative. However, repeated stimulation of V γ 9V δ 2-T cells by phosphoantigens often leads to V γ 9V δ 2-T cell exhaustion.^{23,42,43} An effort to avoid this exhaustion was recently made by another research group, who provided vitamin C during the *ex vivo* expansion of V γ 9V δ 2-T cells.⁴⁴ Here, we further demonstrated that activation of the CD137/CD137L pathway could maintain the survival of V γ 9V δ 2-T cells. The strategy of targeting CD137 costimulation may provide a new solution to avoid V γ 9V δ 2-T cell exhaustion and improve $\gamma\delta$ -T cell-based immunotherapy.

This study improves our understanding of the role of CD137 in the antiviral activity of human $\gamma\delta$ -T cells. It also provides proof-of-concept data for a novel strategy for treating influenza virus infection by targeting CD137 to improve the antiviral activity of human $\gamma\delta$ -T cells and increase the efficacy of $\gamma\delta$ -T cell-based immunotherapy by using the combination of a phosphoantigen and CD137 agonist.

MATERIALS AND METHODS

Generation of PAM-expanded V γ 9V δ 2-T cells and MDMs
PAM-expanded V γ 9V δ 2-T cells were generated as described before.²¹ Briefly, huPBMC were isolated from the buffy coats of healthy donor samples from the Hong Kong Red Cross by Ficoll-Hypaque (Pharmacia, Sweden) gradient centrifugation. The huPBMC were cultured in 10% FBS RPMI-1640 medium with the addition of PAM on day 0 and day 3 at a final concentration of 9 μ g/ml. Recombinant human IL-2 (Invitrogen, USA) was added at a final concentration of 500 IU/ml every 3 days beginning on day 3. After 14 days of culture, V γ 9V δ 2-T cells were purified by negative or positive selection with a $\gamma\delta$ -T cell isolation kit according to the manufacturer's instructions (Miltenyi Biotec, Germany). Human MDMs were generated from mononuclear cells as previously described.¹⁶ In brief, adherent monocytes were seeded in 24-well plates at 5×10^5 cells/well and cultured in RPMI-1640 medium supplemented with 5% autologous serum. Then, they were allowed to differentiate into macrophages for 14 d. The purity of the monocytes, as determined by flow cytometry with an anti-CD14 monoclonal antibody, was consistently >90%.

Purification of CD137⁺ and CD137⁻ V γ 9V δ 2-T cells
PAM-expanded V γ 9V δ 2-T cells were activated with an anti- $\gamma\delta$ -TCR mAb (0.5 μ g/ml) *in vitro* for 6 h, and then the subsets of CD137⁺ and CD137⁻ V γ 9V δ 2-T cells were isolated by selection using the MACS CD137 MicroBead Kit (Miltenyi Biotec, Germany) according to the manufacturer's instructions. The purities of the resulting cell populations were checked routinely by flow cytometry. CD137⁺ and CD137⁻ V γ 9V δ 2-T cells purities generally exceeded 95%.

Preparation of the recombinant SA-hCD137L protein
The DNA sequence encoding core streptavidin (SA; amino acid residues 16-133) and the extracellular domain of human CD137L

(amino acid residues 58-254) with an N-terminal 6 \times His tag was synthesized by Shanghai Sangon Biological Engineering Technology & Services Company Ltd. The DNA fragments were inserted into the pETH expression vector, and the recombinant SA-hCD137L protein was expressed in the *E. coli* strain BL21 (DE3) as an inclusion body after induction at 37 $^{\circ}$ C for 4 h with 0.3 mM IPTG. The inclusion bodies were washed and solubilized with 8 M urea in a TBS solution. After filtering through a 0.45- μ m membrane filter, the protein was purified with Ni-nitrilotriacetic acid affinity chromatography (QIAGEN, Germany) according to the manufacturer's instructions. The purified protein was refolded by dialysis, which gradually removed the urea. Bacterial endotoxin contaminants were removed by using DetoxiGel Endotoxin Removing Gel (Thermo Fisher Scientific, USA). The prepared recombinant SA-hCD137L protein was then filtered through a 0.2- μ m membrane and quantitatively measured with the BCA Protein Assay Kit (Pierce, USA).

Viruses, infections, and treatment of virus-infected humanized and Rag2^{-/-} γ c^{-/-} mice

A mouse-adapted influenza H1N1 (A/PR/8/34) virus was cultured in Madin-Darby canine kidney cells, as described previously.¹⁶ Viral titers were determined by daily observation of the cytopathic effect on cells infected with serial dilutions of virus stock; the median tissue culture infective dose (TCID₅₀) was calculated according to the Reed-Muench formula. For *in vitro* experiments, day 14-differentiated MDMs were infected with influenza virus at a multiplicity of infection (MOI) of 2. After 1 h of viral absorption, the cells were washed with PBS to remove unabsorbed virus. Humanized mice were generated with 4- to 5-week-old male or female Rag2^{-/-} γ c^{-/-} mice by reconstitution with whole huPBMC or V γ 9V δ 2-T cell-depleted huPBMC as we described previously.²¹ Four weeks after huPBMC transplantation, mice were successfully engrafted and became stable with a functional human immune system. Established humanized mice or 6- to 8-week-old Rag2^{-/-} γ c^{-/-} mice were infected intranasally (*i.n.*) with the PR8 virus strain (25 μ l, 10⁴ TCID₅₀) under anesthesia. For Rag2^{-/-} γ c^{-/-} mice, CD137⁺ V γ 9V δ 2-T cells, CD137⁻ V γ 9V δ 2-T cells or whole V γ 9V δ 2-T cells (5×10^6 /mouse) in 200 μ l of PBS were adoptively transferred intravenously (*i.v.*) after infection with PR8 at the indicated time. For humanized mice, SA-hCD137L (15 μ g/mouse) and PAM (5 mg/kg body weight; Pamisol; Hospira NZ) were injected intraperitoneally (*i.p.*) at the indicated time. Mice treated with an equivalent volume of PBS were used as controls. Survival was monitored, and the infected mice were weighed daily. The lungs were collected at the indicated time for viral titer and histology assays.

Cytotoxicity assay

CD137⁺ V γ 9V δ 2-T cells, CD137⁻ V γ 9V δ 2-T cells or whole V γ 9V δ 2-T cells (effector cells, E) were cocultured with PR8-infected MDMs (target cells, T) at an E/T ratio of 10:1 for 6 h. In some experiments, neutralizing antibodies against CD137 (5 μ g/ml, BBK-2, Thermo Fisher Scientific) were used to block CD137-mediated pathways, SA-hCD137L (500 ng/ml) was used to activate CD137-mediated pathways, or mouse IgG1 (5 μ g/ml, MG1-45, BioLegend) or PBS was used as a control. Afterward, nonadherent cells were harvested directly. Adherent cells were detached with 0.25% trypsin-EDTA. All adherent and nonadherent cells were stained with an anti-CD3 antibody to identify V γ 9V δ 2-T cells and ethidium homodimer-2 (EthD-2; Gibco-Life Technologies) to identify dead cells. The cytotoxicity of V γ 9V δ 2-T cells against virus-infected MDMs was assessed by flow cytometry as the percentage of EthD-2⁺ cells in the CD3⁺ population, as we described previously.¹⁶

CFSE assay

Fresh huPBMC (2×10^7 cells) were labeled with 5 μ M carboxy-fluorescein succinimidyl ester (CFSE; Sigma-Aldrich) and then

cultured as described previously to generate PAM-expanded V γ 9V δ 2-T cells. A neutralizing anti-CD137 mAb (5 μ g/ml) was added to block the CD137-mediated signaling pathway, and mouse IgG1 (5 μ g/ml) was used as an isotype control. On day 7, the profile of CFSE in CD3⁺V γ 9⁺ cells was detected by flow cytometry.

Quantification of viral copies by RT-PCR

Viral RNA copies in the lungs of PR8-infected mice were evaluated with a real-time quantitative reverse transcription polymerase chain reaction (qRT-PCR) assay by targeting the conserved matrix gene of influenza virus.⁴⁵ A serially diluted recombinant plasmid (pET-28b(+)/M1) containing the target gene was used as a standard. The lungs from influenza virus-infected mice were harvested at the indicated time and homogenized in PBS. Total RNA was extracted with an RNeasy plus mini kit (QIAGEN) following the manufacturer's instructions. Using the QuantiNova Probe RT-PCR Kit (QIAGEN), one-step qRT-PCR was applied to detect viral RNA with primers (forward primer, 5'-CTTCTAACCGA GGTGCGAACGTA-3'; reverse primer, 5'-GGTGACAGGATTGGTC TTGCTTTA-3') and a TaqMan probe (5'[Fam]-TCAGGCC CCTCAA AGCCGAG-[BHQ-1]3'). The cycling conditions on the ABI Prism 7900HT Fast Real-Time PCR System consisted of 45 °C for 10 min and 95 °C for 5 min, followed by 45 cycles of 95 °C for 5 s and 60 °C for 30 s.

Flow cytometric analysis

Cells were stained for surface markers with the following antibodies (BioLegend): anti-CD3 (HIT3a), anti-TCRV δ 2 (B6), anti-TCR γ 9 (B3), anti-CD25 (BC96), anti-CD69 (FN50), anti-NKG2D (1D11), anti-Fas (DX2), anti-FasL (NOK-1), anti-TRAIL (RIK-2), anti-CD107a (H4A3), anti-CD14 (63D3) and anti-CD137 (4B4-1). For intracellular staining, cells were fixed, permeabilized, and then stained with anti-IFN- γ (B27), anti-perforin (B-D48), anti-granzyme B (QA16A02) and anti-granzyme A (CB9) antibodies or relevant isotype control antibodies as described previously.³¹ All samples were acquired with a FACS LSR II (BD) and analyzed with FlowJo software (Tree Star).

Histological staining and immunohistochemical assays

The lungs of PR8-infected mice were collected at the indicated time, fixed with 10% formalin for 24 h and maintained in 70% ethanol. Paraffin-embedded lungs were sectioned and stained with hematoxylin and eosin.

Statistical analysis

Data are shown as the mean \pm SEM. Multiple regression analysis was used to test the differences in the body weight changes in Rag2^{-/-} γ c^{-/-} mice or humanized mice after infection. The differences in cell death, fluorescence intensity, cell percentages, cell numbers and viral titers between the control and treatment groups were analyzed by an unpaired, two-tailed Student's *t*-test. The *p*-value of the difference in survival was determined by the Kaplan-Meier log-rank test. All these analyses were performed with GraphPad Prism software (version 7.0e, GraphPad software, USA), with *p*-values <0.05 considered significant.

ACKNOWLEDGEMENTS

This work was supported in part by the General Research Fund, Research Grants Council of Hong Kong (17115015, 17121214, 17126317, 17122519); Theme-based Research Scheme from the Research Grants Council of the Hong Kong SAR, China (Project No. T11-705/14N); Chinese National Natural Science Foundation of China (31570898); and Natural Science Foundation of Guangdong Province, China (2016A030313112).

ADDITIONAL INFORMATION

The online version of this article (<https://doi.org/10.1038/s41392-020-0174-2>) contains supplementary material, which is available to authorized users.

Competing interests: The authors declare no competing interests.

REFERENCES

- Bailey, E. S. et al. The continual threat of influenza virus infections at the human-animal interface: what is new from a one health perspective? *Evol. Med. Public Health* **2018**, 192–198 (2018).
- Ziegler, T., Mamahit, A. & Cox, N. J. 65 years of influenza surveillance by a World Health Organization-coordinated global network. *Influenza Other Respir. Viruses* **12**, 558–565 (2018).
- Rebmann, T. & Zelicoff, A. Vaccination against influenza: role and limitations in pandemic intervention plans. *Expert Rev. Vaccines* **11**, 1009–1019 (2012).
- Peiris, J. S. M., Tu, W.-w & Yen, H.-I. A novel H1N1 virus causes the first pandemic of the 21st century. *Eur. J. Immunol.* **39**, 2946–2954 (2009).
- McKimm-Breschkin, J. L. Influenza neuraminidase inhibitors: antiviral action and mechanisms of resistance. *Influenza Other Respir. Viruses* **7**, 25–36 (2013).
- Leung, K., Lipsitch, M., Yuen, K. Y. & Wu, J. T. Monitoring the fitness of antiviral-resistant influenza strains during an epidemic: a mathematical modelling study. *Lancet Infect. Dis.* **17**, 339–347 (2017).
- Hussain, M. et al. Drug resistance in influenza A virus: the epidemiology and management. *Infect. Drug Resist.* **10**, 121–134 (2017).
- Wang, B. X. & Fish, E. N. Global virus outbreaks: Interferons as 1st responders. *Semin. Immunol.* **43**, 101300 (2019).
- Zheng, J., Liu, Y., Lau, Y. L. & Tu, W. gammadelta-T cells: an unpolished sword in human anti-infection immunity. *Cell Mol. Immunol.* **10**, 50–57 (2013).
- Zhu, Y. et al. miR-125b-5p and miR-99a-5p downregulate human gammadelta T-cell activation and cytotoxicity. *Cell Mol. Immunol.* **16**, 112–125 (2019).
- Bonneville, M., O'Brien, R. L. & Born, W. K. Gammadelta T cell effector functions: a blend of innate programming and acquired plasticity. *Nat. Rev. Immunol.* **10**, 467–478 (2010).
- Born, W. K., Reardon, C. L. & O'Brien, R. L. The function of gammadelta T cells in innate immunity. *Curr. Opin. Immunol.* **18**, 31–38 (2006).
- Beetz, S. et al. Innate immune functions of human gammadelta T cells. *Immunobiology* **213**, 173–182 (2008).
- Bonneville, M. & Scotet, E. Human Vgamma9Vdelta2 T cells: promising new leads for immunotherapy of infections and tumors. *Curr. Opin. Immunol.* **18**, 539–546 (2006).
- Urban, E. M., Chapoval Ai Fau - Pauza, C. D. & Pauza, C. D. Repertoire development and the control of cytotoxic/effector function in human gammadelta T cells. *Clin. Dev. Immunol.* **2010**, 732893 (2010).
- Qin, G. et al. Phosphoantigen-expanded human gammadelta T cells display potent cytotoxicity against monocyte-derived macrophages infected with human and avian influenza viruses. *J. Infect. Dis.* **200**, 858–865 (2009).
- Qin, G. et al. Type 1 responses of human Vgamma9Vdelta2 T cells to influenza A viruses. *J. Virol.* **85**, 10109–10116 (2011).
- Qin, G. et al. Phenotypic and functional characterization of human gammadelta T-cell subsets in response to influenza A viruses. *J. Infect. Dis.* **205**, 1646–1653 (2012).
- Li, H. et al. Human Vgamma9Vdelta2-T cells efficiently kill influenza virus-infected lung alveolar epithelial cells. *Cell Mol. Immunol.* **10**, 159–164 (2013).
- Chen, Q. et al. Human Vgamma9Vdelta2-T cells synergize CD4(+) T follicular helper cells to produce influenza virus-specific antibody. *Front. Immunol.* **9**, 599 (2018).
- Tu, W. et al. The aminobisphosphonate pamidronate controls influenza pathogenesis by expanding a gammadelta T cell population in humanized mice. *J. Exp. Med.* **208**, 1511–1522 (2011).
- Zheng, J. et al. The therapeutic effect of pamidronate on lethal avian influenza A H7N9 virus infected humanized mice. *PLoS ONE* **10**, e0135999 (2015).
- Sicard, H. et al. In vivo immunomanipulation of V γ 9V δ 2 T cells with a synthetic phosphoantigen in a preclinical nonhuman primate model. *J. Immunol.* **175**, 5471–5480 (2005).
- Chester, C., Ambulkar, S. & Kohrt, H. E. 4-1BB agonism: adding the accelerator to cancer immunotherapy. *Cancer Immunol. Immunother.* **65**, 1243–1248 (2016).
- Uno, T. et al. Eradication of established tumors in mice by a combination antibody-based therapy. *Nat. Med.* **12**, 693–698 (2006).
- Melero, I. et al. Monoclonal antibodies against the 4-1BB T-cell activation molecule eradicate established tumors. *Nat. Med.* **3**, 682–685 (1997).

27. Zhao, Y., Shao, Q. & Peng, G. Exhaustion and senescence: two crucial dysfunctional states of T cells in the tumor microenvironment. *Cell Mol. Immunol.* **17**, 27–35 (2020).
28. Halstead, E. S., Mueller Ym Fau - Altman, J. D., Altman Jd Fau - Katsikis, P. D. & Katsikis, P. D. In vivo stimulation of CD137 broadens primary antiviral CD8+ T cell responses. *Nat. Immunol.* **3**, 536–541 (2002).
29. Munks, M. W. et al. 4-1BB and OX40 stimulation enhance CD8 and CD4 T-cell responses to a DNA prime, poxvirus boost vaccine. *Immunology* **112**, 559–566 (2004).
30. Rubio, V. et al. Ex vivo identification, isolation and analysis of tumor-cytolytic T cells. *Nat. Med.* **9**, 1377–1382 (2003).
31. Xiang, Z. et al. Targeted activation of human Vgamma9Vdelta2-T cells controls epstein-barr virus-induced B cell lymphoproliferative disease. *Cancer Cell.* **26**, 565–576 (2014).
32. Ni, K. et al. PD-1/PD-L1 Pathway mediates the alleviation of pulmonary fibrosis by human mesenchymal stem cells in humanized mice. *Am. J. Respir. Cell Mol. Biol.* **58**, 684–695 (2018).
33. Bertram, E. M., Lau P Fau - Watts, T. H. & Watts, T. H. Temporal segregation of 4-1BB versus CD28-mediated costimulation: 4-1BB ligand influences T cell numbers late in the primary response and regulates the size of the T cell memory response following influenza infection. *J. Immunol.* **168**, 3777–3785 (2002).
34. Lin, G. H. et al. Endogenous 4-1BB ligand plays a critical role in protection from influenza-induced disease. *J. Immunol.* **182**, 934–947 (2009).
35. Zhao, Y., Tahiliani, V., Salek-Ardakani, S. & Croft, M. Targeting 4-1BB (CD137) to enhance CD8 T cell responses with poxviruses and viral antigens. *Front. Immunol.* **3**, 332 (2012).
36. Shuford, W. W. et al. 4-1BB costimulatory signals preferentially induce CD8+ T cell proliferation and lead to the amplification in vivo of cytotoxic T cell responses. *J. Exp. Med.* **186**, 47 LP-47 55 (1997).
37. Lee, S. J. et al. 4-1BB signal stimulates the activation, expansion, and effector functions of $\gamma\delta$ T cells in mice and humans. *Eur. J. Immunol.* **43**, 1839–1848 (2013).
38. Lin, G. H. et al. GITR-dependent regulation of 4-1BB expression: implications for T cell memory and anti-4-1BB-induced pathology. *J. Immunol.* **190**, 4627–4639 (2013).
39. Ascierto, P. A. et al. Clinical experiences with anti-CD137 and anti-PD1 therapeutic antibodies. *Semin. Oncol.* **37**, 508–516 (2010).
40. Barsoumian, H. B. et al. A novel form of 4-1BBL prevents cancer development via nonspecific activation of CD4(+) T and natural killer cells. *Cancer Res.* **79**, 783–794 (2019).
41. Srivastava, A. K. et al. SA-4-1BBL and monophosphoryl lipid A constitute an efficacious combination adjuvant for cancer vaccines. *Cancer Res.* **74**, 6441–6451 (2014).
42. Dieli, F. et al. Targeting human $\gamma\delta$ T cells with zoledronate and interleukin-2 for immunotherapy of hormone-refractory prostate cancer. *Cancer Res.* **67**, 7450 (2007).
43. Braza, M. S. & Klein, B. Anti-tumour immunotherapy with V γ 9V δ 2 T lymphocytes: from the bench to the bedside. *Br. J. Haematol.* **160**, 123–132 (2013).
44. Kouakanou, L. et al. Vitamin C promotes the proliferation and effector functions of human gammadelta T cells. *Cell Mol. Immunol.* <https://doi.org/10.1038/s41423-019-0247-8> (2019)
45. Liu, Y. et al. Uncompromised NK cell activation is essential for virus-specific CTL activity during acute influenza virus infection. *Cell Mol. Immunol.* **15**, 827–837 (2018).



Open Access This article is licensed under a Creative Commons Attribution 4.0 International License, which permits use, sharing, adaptation, distribution and reproduction in any medium or format, as long as you give appropriate credit to the original author(s) and the source, provide a link to the Creative Commons license, and indicate if changes were made. The images or other third party material in this article are included in the article's Creative Commons license, unless indicated otherwise in a credit line to the material. If material is not included in the article's Creative Commons license and your intended use is not permitted by statutory regulation or exceeds the permitted use, you will need to obtain permission directly from the copyright holder. To view a copy of this license, visit <http://creativecommons.org/licenses/by/4.0/>.

© The Author(s) 2020